Online Supplemental Material

Figure S1. Colocalization of *At*MAP65-1 and *At*MAP65-5 with microtubule bundles observed by fluorescent microscopy. Rhodamine-labelled taxol-stabilized MTs (1μM) were incubated in the presence of GFP-*At*MAP65-1 (a, b, c) and GFP-*At*MAP65-5 (d, e, f) at 0.5 μM for 20 min at room temperature. (a, b) observations in the rhodamine channel, (b, e) observations in the GFP channel and (c, f) merge of the rhodamine and GFP images. Bar: 10 μm.

Figure S2. Identification of the MT binding domain of *At*MAP65-1 and *At*MAP65-5. Co-sedimentation of 1 μM of *At*MAP65-1 **(A)** and *At*MAP65-5 **(B)** constructs with MTs (5 μM) *in vitro*. *At*MAP65-1 and -5, *At*MAP65(2), *At*MAP65(3), *At*MAP65(23), *At*MAP65(13), *At*MAP65-5(Δ3C) and *At*MAP65(3C) were centrifuged at high speed and protein content of pellets (P) and supernatant (S) were analysed on western blot probed with anti-*At*MAP65-1 or anti-*At*MAP65-5. Only the constructs *At*MAP65(2) and *At*MAP65(3C) did not sedimented with MTS. These data demonstrate that the MT binding domain is located within the domain 3N for both *At*MAP65-1 and *At*MAP65-5.

Figure S3. Tubulin assembly *in vitro*. Time-course assembly of tubulin (15 μM) followed at 350 nm in the presence of various concentrations of *At*MAP65-1 (top-left panel), *At*MAP65-1(Δ3C) (top-right panel), *At*MAP65-5 (bottom-left panel), and *At*MAP65-5(Δ3C) (bottom-right panel).

Video 1. Tobacco BY-2 cells expressing *At*MAP65-5-GFP and RFP-TUA6 undergoing from prophase to telophase. The movie corresponds to the merged of RFP and GFP images

(confocal microscopy). This movie is from experiment shown in Figure 7A. Frames were collected every 3 min and the video is shown at 30msec/frames.

Video 2. Tobacco BY-2 cells expressing *At*MAP65-5-GFP and RFP-TUA6 undergoing division from prophase to telophase. The movie corresponds to the merged RFP and GFP images (confocal microscopy). This movie is from experiment shown in Figure 6B. Frames were collected every 3 min and the video is shown at 30msec/frame.

Video 3. Tobacco BY-2 cells expressing *At*MAP65-1-GFP and RFP-TUA6 undergoing division from metaphase to telophase. The movie corresponds to the merged RFP and GFP images (confocal microscopy). This movie is from experiments shown in Figure 7B. Frames were collected every 3 min and the video is shown at 30msec/frame.

Table I. Sequences of the primers used for cloning *At*MAP65s.

Supplementary Material and Methods

Expression and purification of recombinant MAP65s

His-*At*MAP65s-His proteins were expressed for 16h at 22°C in Rosetta (DE3)pLysS bacteria strain (Novagen-Merck Biosciences) by induction with 0.5 mM IPTG. After induction, cells were suspended in cold lysis buffer (50 mM NaPi, 0.1 M NaCl, 0.5 mM DTT, 0.5% TritonX100, 30 mM Imidazole, pH 7.9), containing protease inhibitors (complete, EDTAfree, Roche) and sonicated. Cell lysate was centrifuged at 30,000*g* for 30 min and applied to Ni Sepharose columns (Amersham Bioscience). Columns were washed with protein wash buffer

(50 mM NaPi, 0.1 M NaCl, 0.5 mM DTT, 0.12 M Imidazole, pH 7.9). Proteins were eluted with 0.5 M Imidazole, and dialyzed overnight against the dialysing buffer (50 mM NaPi, 0.1 M NaCl, 0.5 mM DTT). To purified His-*At*MAP65s-GFP proteins, the same protocol was applied except that the protein wash buffer contained 30 mM Imidazole and the proteins were eluted with 0.5 M Imidazole. The affinity purification was followed by a gel filtration chromatography in 50 mM NaPi, 0.1 M NaCl, 0.5 mM DTT, pH 7.9. Purified *At*MAP65s were frozen in liquid nitrogen in the presence of 10% of glycerol and store at –80°C. Recombinant proteins were analyzed on a 10% SDS-PAGE slab gel stained with Coomassie Brillant Blue R-250 (Sigma-Aldrich). The amount of protein was evaluated by scanning the gel with NIH IMAGE software (http://rsb.info.nih.gov/nih-image/), with actin as standard protein.

Oligomerization determination

Corrected $s_{20,w}$ sedimentations coefficients were derived from s: $s_{20,w}=s$ ((1-0.99828$\bar{v}$)/ (1-$\rho\bar{v}$))(η/1.002). The partial specific volume of the proteins were estimated from the sequence $\bar{v}$ =0.730±0.002 mL.g^{-1}; the solvent density was measured: ρ =1.039 ± 0.001 mL.g^{-1}.Theorerical calculations were made with the Svedberg equation: $s = M(1-\rho\bar{v})/(N_A 6 \pi \eta R_H)$ with $R_H = (f/f_{min}) R_{min}$). N_A Avogadro's number, R_{min} is the radius corresponding to the volume of a molecule; (f/f_{min}) is the frictional ratio. (f/f_{min}) is 1.25 for globular proteins For the range of our molar mass, we derive (f/f_{min})~2.5 for coil-like- and (f/f_{min})~1.7 for premolten globule-like- unfolded proteins (Ebel, 2007). For gel filtration chromatography, the column was calibrated by both high and low molecular weight standards (Amersham Biosciences).

Details of the methodology employed for microtubule polarity analysis

Because of the distorsion of the MTs (that we may not control), the computation of the filtered

images using the J0 and JN terms in the Fourier transform of the images shows blury features. To avoid this artefact we had to compute filtered images for the straightest part of MTs, and statistically only small portions of MTs are straight in most cases. Furthermore, MTs in presence of *At*MAP65s involve the formation of MTs bundles in 3D. That means that MTs in interaction with *At*MAP65s in (only) "2D" is a rare phenomenon (see Figure 5Ab and 5Bb). During this study over 210 images of MT bundles induced by *At*MAP65-1 were recorded and only 17 MTs in interaction with *At*MAP65-1 and without any overlapp in the third dimension (less than 10%) could be analyzed; for MT bundles induced by *At*MAP65-5, 330 images were recorded, 38 of those showed MTs in interaction with *At*MAP65-5 without any overlapp in the third dimension (a little bit more than 10% in this case). Once these images were selected, and before applying the method for the polarity determination, we had to ensure that MTs were really in interaction with *At*MAP65s (and that they are not just undecorated MTs) by performing a Fourier transform of a part of the area of interest. If an extra layer-line at ~1/8 nm appeared, it confirmed the binding of *At*MAP65s (see Figure 5Ae and Be). If no extra layer-line was visible, either MT was undecorated or the signal was lost in the noise (cryo-EM images have a very poor signal to noise ratio). Taking into account these last restrictive experimental conditions and in order to apply the method described by Chrétien et al., (1996) we furthermore had to select MTs with a number of protofilaments which was not 13, MTs with 13 protofilaments representing more than 70% of our MTs population. In conclusion, we determined the polarity of 5 MTs interacting with *At*MAP65-1 over the 17 first selected images and 4 over the 38 selected images for *At*MAP65-5 as presented in Figure 5Ab-e (i.e evidence of the binding of *At*MAP65-1 and at least 2 neighbouring MTs with a number of protofilaments different from 13).

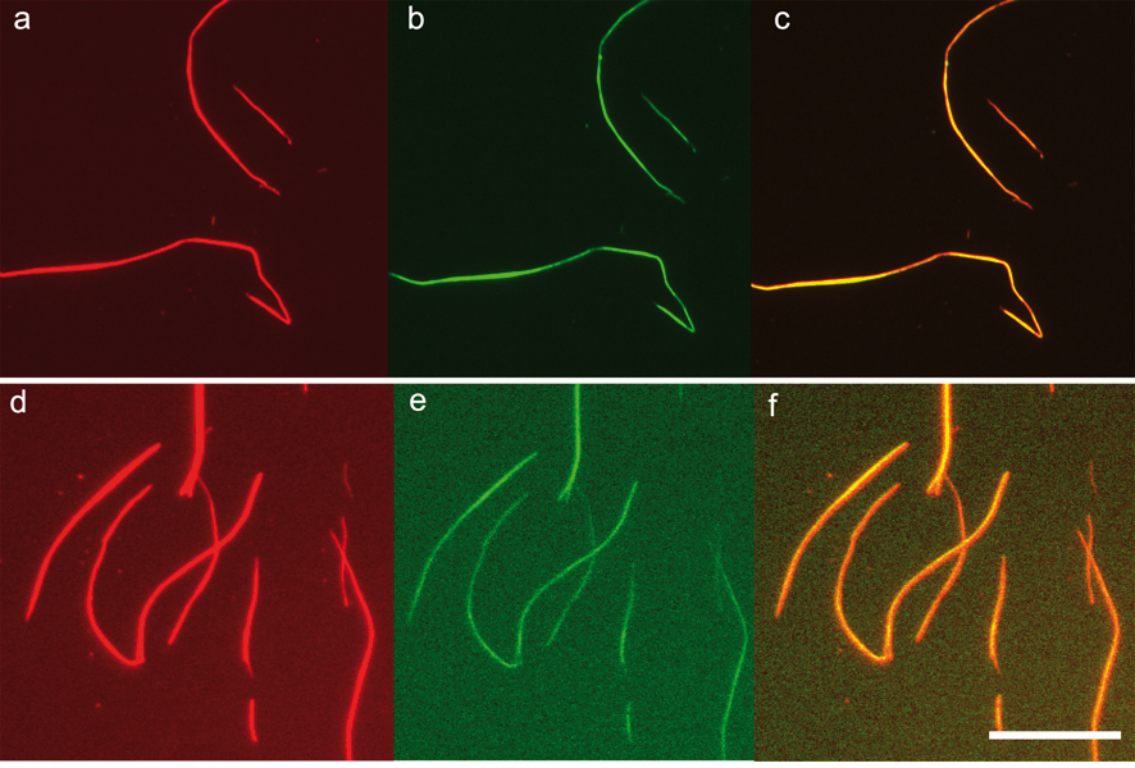

Figure S1

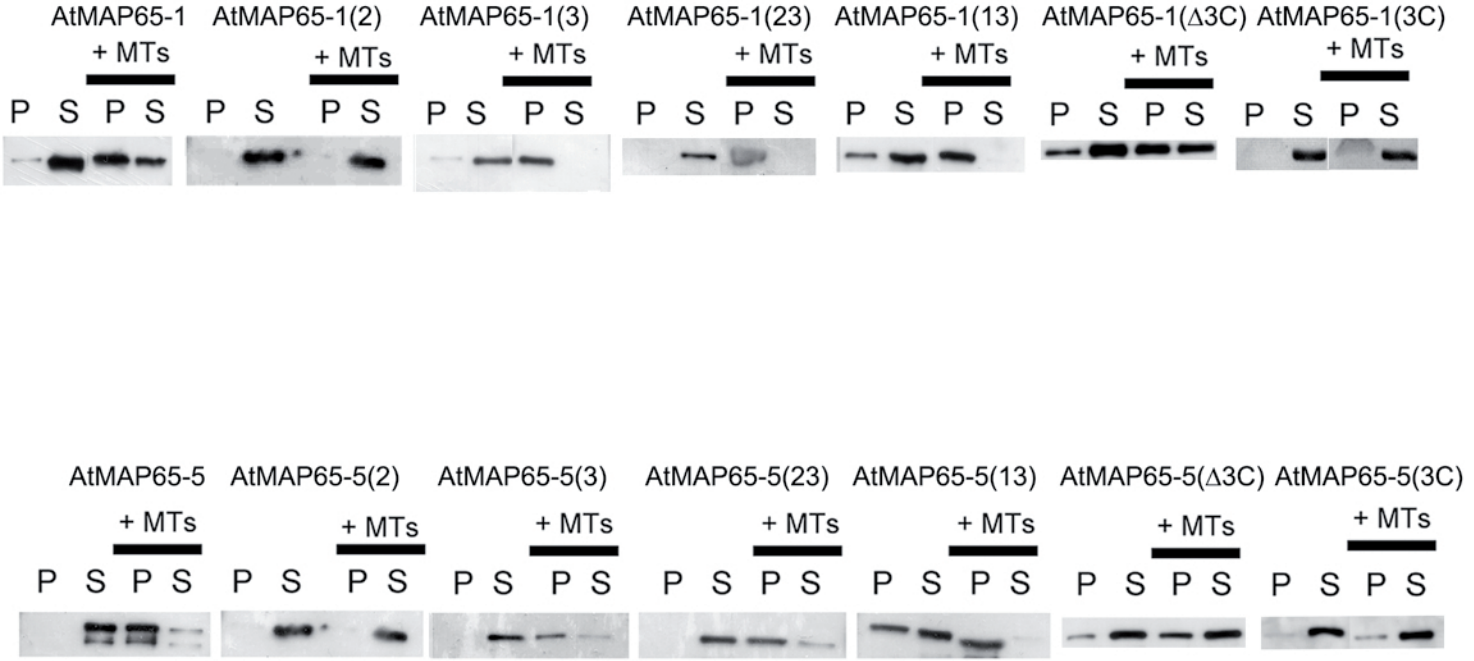
AtMAP65-1
+ MTs
P S P S
AtMAP65-1(2)
+ MTs
P S P S
AtMAP65-1(3)
+ MTs
P S P S
AtMAP65-1(23)
+ MTs
P S P S
AtMAP65-1(13)
+ MTs
P S P S
AtMAP65-1(Δ3C)
+ MTs
P S P S
AtMAP65-1(3C)
+ MTs
P S P S
AtMAP65-5
+ MTs
P S P S
AtMAP65-5(2)
+ MTs
P S P S
AtMAP65-5(3)
+ MTs
P S P S
AtMAP65-5(23)
+ MTs
P S P S
AtMAP65-5(13)
+ MTs
P S P S
AtMAP65-5(Δ3C)
+ MTs
P S P S
AtMAP65-5(3C)
+ MTs
P S P S

Figure S2

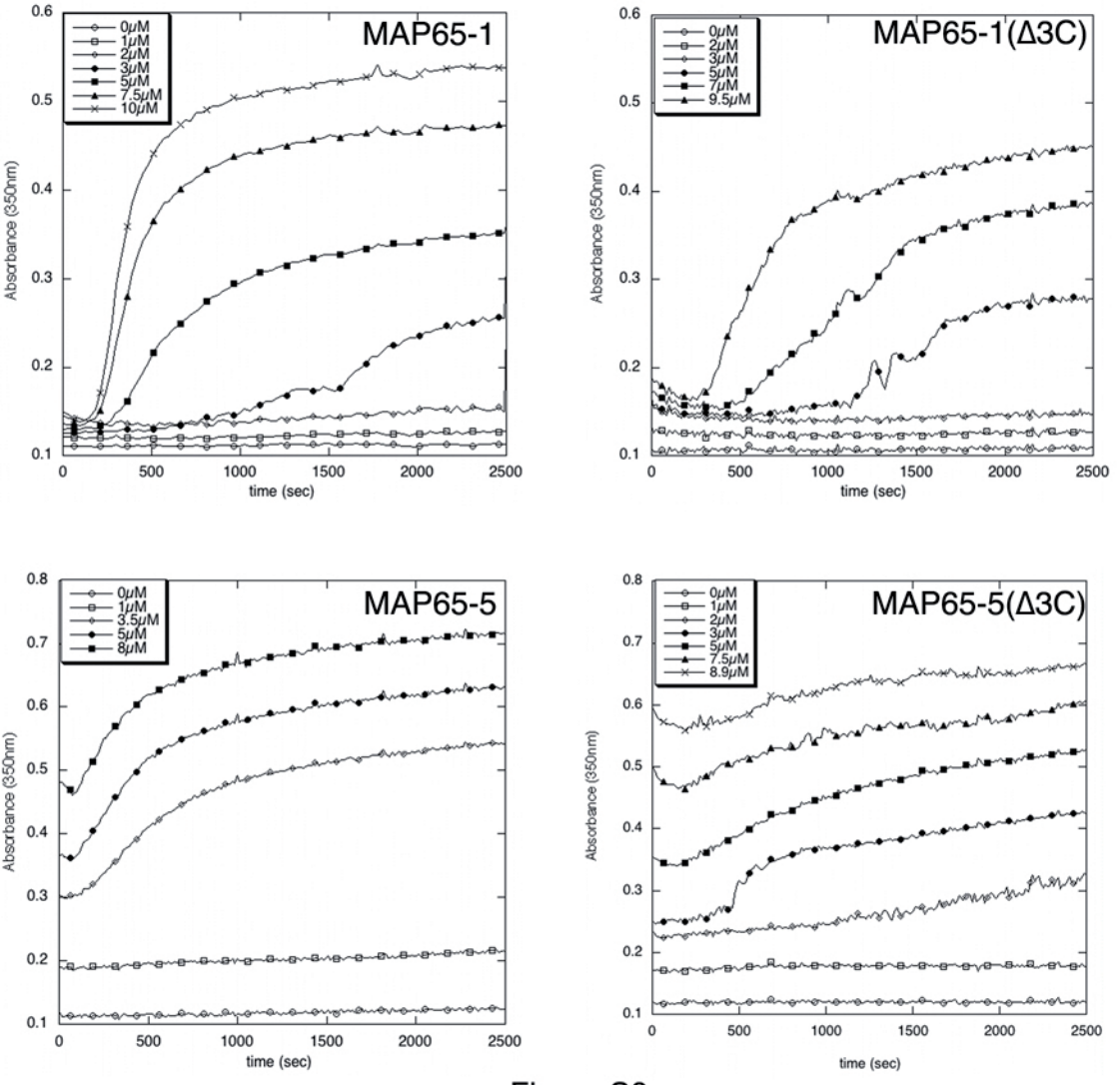
MAP65-1
0μM
1μM
2μM
3μM
5μM
7.5μM
10μM
MAP65-1(Δ3C)
0μM
2μM
3μM
5μM
7μM
9.5μM
MAP65-5
0μM
1μM
3.5μM
5μM
8μM
MAP65-5(Δ3C)
0μM
1μM
2μM
3μM
5μM
7.5μM
8.9μM
Absorbance (350nm)
time (sec)

Figure S3

Table I

Clone	Sequence of the primers
*At*MAP65-1(2)	ForM65-1(2) CACCGATGAGTCTGATTTGTCACTGAAGA RevM65-1(2) TTCCGGGTTAACTTCTACATGGGC
*At*MAP65-1(3)	ForM65-1(3) CACCTCTGCTCGTGAGAGAATCATGT RevM65-1 TGGTGAAGCTGGAACTTGATGAT
*At*MAP65-1(23)	ForM65-1(2) RevM65-1
*At*M65-1(13)	1st PCR to amplify the domain 1: ForM65.1 CACCATGGCAGTTACAGATACTGAAAG RevM65-1(13int) TCTCTCACGAGCAGAGACTATAGGAACCTCATTGCTCA 2nd PCR to amplify the domain 3 ForM65-1(13int) GAGGTTCCTATAGTCTCTGCTCGTGAGAGAATCATGT RevM65-1 3rd PCR to join the two domains with primers ForM65-1 and RevM65-1, taking advantage of the overlapping region introduced during the first amplification.
*At*M65-1(Δ3C)	ForM65.1 RevM65.1(D3C) TCTTGCAGGGCTTGGCCTGGT
*At*M65-1(3C)	ForM65.1(3C) CACCCACAGCATGTCCTTTGCCTA RevM65.1
*At*M65-1(3N)	ForM65.1(3) and RevM65.1(D3C)
*At*MAP65-5(2)	ForM65-5(2) CACCGAAGTTGATGAAAGTGACTTGACACA RevM65-5(2) GATATCCATATGATTCCCTCTGCA-3’
*At*MAP65-5(3)	ForM65-*5*(3) CACCAATAGTGATGCTGCAAGAAAGAGTCT RevM65-5 ATCGTCTTTCTGAAGAGCAACATA
*At*MAP65-5(23)	ForM65-*5*(2) and RevM65-*5*.
*At*MAP65-1(13)	1st PCR to amplify the domain 1 ForM65-*5* CACCATGTCTCCGTCTTCAACCACTA RevM65-*5*(13int) TGCAGCATCACTATTTGAACCAGAACTAACAGTATAATCATTCC 2nd PCR to amplify the domain 3 ForM65-5(13int) GTTAGTTCTGGTTCAAATAGTGATGCTGCAAGAAAGAGTCT RevM65-5 3rd PCR to join the two domains with primers ForM65-5 and RevM65-5, taking advantage of the overlapping region introduced during the first amplification.
*At*M65-5(Δ3C)	ForM65.5 RevM65.1(D3C) AGACTTGGAACCATACTTTGCTTCTTTC
*At*M65-5(3C)	ForM65.5(3C) CACCAGAGGGGTCCCCTTCTTATGC RevM65.5
*At*M65-5(3N)	ForM65.5(3) and RevM65.5(D3C)